

AD-A136 461

THE PERFORMANCE OF AN LMS (LEAST MEAN SQUARE) ADAPTIVE
ARRAY WITH FREQUEN. (U) OHIO STATE UNIV COLUMBUS
ELECTROSCIENCE LAB L ACAR ET AL. JUN 83 ESL-714505-5

1/1

UNCLASSIFIED

N00019-82-C-0190

F/G 9/5

NL

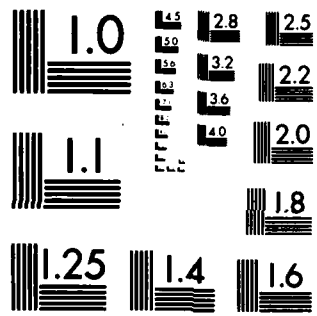
END

DATE

FORMED

2884

DTIC



MICROCOPY RESOLUTION TEST CHART
NATIONAL BUREAU OF STANDARDS-1963-A

13

OSU

The Ohio State University

**THE PERFORMANCE OF AN LMS ADAPTIVE ARRAY
WITH FREQUENCY HOPPED SIGNALS**

Levent Acar
R.T. Compton, Jr.

A136461

The Ohio State University

ElectroScience Laboratory

Department of Electrical Engineering
Columbus, Ohio 43212

Technical Report 714505-5

Contract N00019-82-C-0190

June 1983

DTIC
ELECTE
DEC 28 1983
A

FILE COPY

Department of the Navy
Naval Air Systems Command
Washington, D.C. 20361

APPROVED FOR PUBLIC RELEASE
DISTRIBUTION UNLIMITED

83 12 28 016

NOTICES

When Government drawings, specifications, or other data are used for any purpose other than in connection with a definitely related Government procurement operation, the United States Government thereby incurs no responsibility nor any obligation whatsoever, and the fact that the Government may have formulated, furnished, or in any way supplied the said drawings, specifications, or other data, is not to be regarded by implication or otherwise as in any manner licensing the holder or any other person or corporation, or conveying any rights or permission to manufacture, use, or sell any patented invention that may in any way be related thereto.

REPORT DOCUMENTATION PAGE		1. REPORT NO.	2.	3. Recipient's Accession No.
4. Title and Subtitle THE PERFORMANCE OF AN LMS ADAPTIVE ARRAY WITH FREQUENCY HOPPED SIGNALS			5. Report Date June 1983	6.
7. Author(s) Levent Acar and R.T. Compton, Jr.			8. Performing Organization Rept. No. ESL 714505-5	
9. Performing Organization Name and Address The Ohio State University ElectroScience Laboratory Department of Electrical Engineering Columbus, Ohio 43212			10. Project/Task/Work Unit No.	
			11. Contract(C) or Grant(G) No. (C) (G) N00019-82-C-0190	
12. Sponsoring Organization Name and Address Department of the Navy, Naval Air Systems Command Washington, D.C. 20361			13. Type of Report & Period Covered Technical Report	
			14.	
15. Supplementary Notes				
16. Abstract (Limit: 200 words) <p>This report examines the performance of an LMS adaptive array with a frequency hopped, spread spectrum desired signal and a CW interference signal. It is shown that frequency hopping has several effects on an adaptive array. It causes the array to modulate both the amplitude and the phase of the received signal. Also, it causes the array output SINR (signal-to-interference-plus-noise ratio) to vary with time and thus increases the bit error probability for the received signal. Typical curves of the desired signal modulation and the time-varying SINR at the array output are presented. It is shown how the array performance depends on hopping frequency, frequency jump size, interference frequency, signal arrival angles and signal powers.</p>				
17. Document Analysis a. Descriptors <p>arrays adaptive arrays interference rejection</p> <p>spread spectrum frequency hopping</p> <p>b. Identifiers/Open-Ended Terms</p> <p>c. GDBAT/ Field/Group</p>				
18. Availability Statement APPROVED FOR PUBLIC RELEASE: DISTRIBUTION UNLIMITED		19. Security Class (This Report) Unclassified		20. No. of Pages 49
		20. Security Class (This Page) Unclassified		22. Price

LIST OF FIGURES

Figure	Page
1. A Three-Element Adaptive Array.	4
2. <u>Desired Signal Amplitude vs. Time</u> $\theta_d = 15^\circ, \theta_i = 30^\circ, \xi_d = 6 \text{ dB}, \xi_i = 20 \text{ dB}.$ $p = 2, B_r = 0.1, \omega_i = \omega_1.$	18
3. <u>Array Patterns During Hopping Period</u> $\theta_d = 15^\circ, \theta_i = 30^\circ, \xi_d = 6 \text{ dB}, \xi_i = 20 \text{ dB}.$ $p = 2, B_r = 0.1, \omega_i = \omega_1.$ Patterns computed at $\omega_2.$	18
4. <u>Desired Signal Phase Angle vs. Time</u> $\theta_d = 15^\circ, \theta_i = 45^\circ, \xi_d = 6 \text{ dB}, \xi_i = 20 \text{ dB},$ $p = 2, B_r = 0.5, \omega_i = \omega_1.$	21
5. <u>Desired Signal Phase Angle vs. Time</u> $\theta_d = 15^\circ, \xi_d = 6 \text{ dB}, p = 2, B_r = 0.5,$ no interference.	21
6. <u>SINR vs. Time</u> $\theta_d = 15^\circ, \theta_i = 30^\circ, \xi_d = 6 \text{ dB}, \xi_i = 20 \text{ dB},$ $p = 2, B_r = 0.1, \omega_i = \omega_1.$	24
7. <u>Envelope Variation vs. Pattern Frequency</u> $\theta_d = 15^\circ, \theta_i = 45^\circ, \xi_d = 6 \text{ dB}, \xi_i = 40 \text{ dB},$ $p = 2, \omega_i = \omega_1.$	24
8. <u>Phase Variation vs. Pattern Frequency</u> $\theta_d = 15^\circ, \theta_i = 45^\circ, \xi_d = 6 \text{ dB}, \xi_i = 40 \text{ dB},$ $p = 2, \omega_i = \omega_1.$	27
9. <u>Bit Error Probability vs. Pattern Frequency</u> $\theta_d = 15^\circ, \theta_i = 45^\circ, \xi_d = 6 \text{ dB}, \xi_i = 40 \text{ dB},$ $p = 2, \omega_i = \omega_1.$	27
10. <u>Bit Error Probability vs. Pattern Frequency</u> $\theta_d = 15^\circ, \theta_i = 45^\circ, \xi_d = 6 \text{ dB}, \xi_i = 40 \text{ dB},$ $p = 3, \omega_i = \omega_1.$	30
11. <u>Bit Error-Probability vs. Pattern Frequency</u> $\theta_d = 15^\circ, \theta_i = 45^\circ, \xi_d = 6 \text{ dB}, \xi_i = 40 \text{ dB},$ $p = 3, \omega_i = \omega_2.$	30

Figure	Page
12. <u>Envelope Variation vs. Pattern Frequency</u> $\theta_d = 15^\circ, \xi_d = 6 \text{ dB}, \xi_f = 40 \text{ dB}, p = 2,$ $B_r = 0.1, \omega_f = \omega_1.$	32
13. <u>Envelope Variation vs. Pattern Frequency</u> $\theta_d = 15^\circ, \xi_d = 6 \text{ dB}, \xi_f = 40 \text{ dB}, p = 2,$ $B_r = 0.1, \omega_f = \omega_1.$	32
14. <u>Phase Variation vs. Pattern Frequency</u> $\theta_d = 15^\circ, \xi_d = 6 \text{ dB}, \xi_f = 40 \text{ dB}, p = 2,$ $B_r = 0.5, \omega_f = \omega_1.$	33
15. <u>Bit Error Probability vs. Pattern Frequency</u> $\theta_d = 15^\circ, \xi_d = 6 \text{ dB}, \xi_f = 40 \text{ dB}, p = 2,$ $B_r = 0.1, \omega_f = \omega_1.$	33
16. <u>Envelope Variation vs. Pattern Frequency</u> $\theta_d = 15^\circ, \theta_f = 45^\circ, \xi_d = 6 \text{ dB}, p = 2,$ $B_r = 0.1, \omega_f = \omega_1.$	35
17. <u>Bit Error Probability vs. Pattern Frequency</u> $\theta_d = 15^\circ, \theta_f = 45^\circ, \xi_d = 6 \text{ dB}, p = 2,$ $B_r = 0.1, \omega_f = \omega_1.$	35
18. <u>Phase Variation vs. Pattern Frequency</u> $\theta_d = 15^\circ, \theta_f = 45^\circ, \xi_d = 6 \text{ dB}, p = 2,$ $B_r = 0.5, \omega_f = \omega_1.$	36
19. <u>Bit Error Probability vs. Pattern Frequency</u> $\theta_d = 15^\circ, \theta_f = 45^\circ, \xi_f = 40 \text{ dB}, p = 2,$ $B_r = 0.1, \omega_f = \omega_1.$	36

1. INTRODUCTION

Adaptive arrays based on the LMS (least mean square) algorithm [1] are very effective for protecting communication systems from interference. These antennas can automatically track desired signals while also nulling interference [2]. Methods have been developed for using adaptive arrays with ordinary AM (amplitude modulated) signals [3], binary FSK (frequency shift keyed) signals [4, 5, 6], binary PSK (phase shift keyed) spread spectrum signals [4, 7], and quadrature PSK spread spectrum signals [8]. These techniques have all been demonstrated experimentally.

In this report we study the performance of an adaptive array with another type of spread spectrum signal, a frequency hopped signal [9]. Frequency hopping is a widely used method of spectrum spreading. Its purpose is also to make a communication system less vulnerable to interference. For some applications, it may be desirable to combine adaptive arrays with frequency hopped signals to obtain the interference protection of both.

However, very little information is available on the performance of adaptive arrays with frequency hopped signals. As we shall show in this report, frequency hopping has several adverse effects on an LMS array. First, it causes the array to modulate both the amplitude and the phase of the received signal. Second, it makes the output SINR (signal-to-interference-plus-noise ratio) vary with time and hence increases the bit error probability for the demodulated signal. If an LMS array is to be used with frequency hopped signals, these effects

must be taken into account in the design of both the array and the signal modulation.

In this report we consider an ordinary LMS adaptive array with continuous feedback loops. We do not consider various modifications of the LMS array (such as weight storage and recall algorithms) that might be used to improve its performance with frequency hopped signals. Our purpose here is to determine when the basic LMS array has problems and to characterize the array behavior with frequency hopped signals.

We use a simple model to study this problem. We consider an array with three elements, and we assume the frequency hopped signal has only a few frequencies. Such a model is adequate to illustrate the effects of frequency hopping on the array, and it allows us to explore the interaction between the hopping characteristics and the array transients.

Section II of the report defines the problem and formulates a method for calculating array behavior with frequency hopped signals. Section III describes numerical results based on the technique in Section II. Section IV contains the conclusions.

II. FORMULATION

Consider an LMS adaptive array [1] with three elements, as shown in Figure 1. Let the elements be isotropic, noninteracting and a half wavelength apart at the center frequency of the signals. The analytic signal $\tilde{y}_j(t)$ from the j th element is mixed with a local oscillator (LO) and then passed through a narrowband filter (NBF). The purpose of the LO and NBF is to dehop the desired signal, as will be discussed below. The filter output $\tilde{x}_j(t)$ is the input to the j th channel of an LMS processor [1]. This processor multiplies each signal $\tilde{x}_j(t)$ by a complex weight w_j and then sums the result to form the array output $\tilde{s}(t)$. The weights w_j in an LMS processor are obtained by correlation feedback loops that minimize the average power in the error signal $\tilde{e}(t)$ [3]. $\tilde{e}(t)$ is the difference between the reference signal $\tilde{r}(t)$ and the array output $\tilde{s}(t)$. The reference signal determines which signals are to be retained in the array output and which are to be nulled. Received signals correlated with $\tilde{r}(t)$ will be retained and signals uncorrelated with $\tilde{r}(t)$ will be nulled. In practical communication systems, $\tilde{r}(t)$ is usually derived from the array output by nonlinear signal processing operations [4-8]. In this report, we do not address the problem of reference signal generation. We simply assume $\tilde{r}(t)$ to be a signal correlated with the desired signal.

Let $Y(t)$ be a vector containing the element signals,

$$Y(t) = [\tilde{y}_1(t), \tilde{y}_2(t), \tilde{y}_3(t)]^T, \quad (1)$$

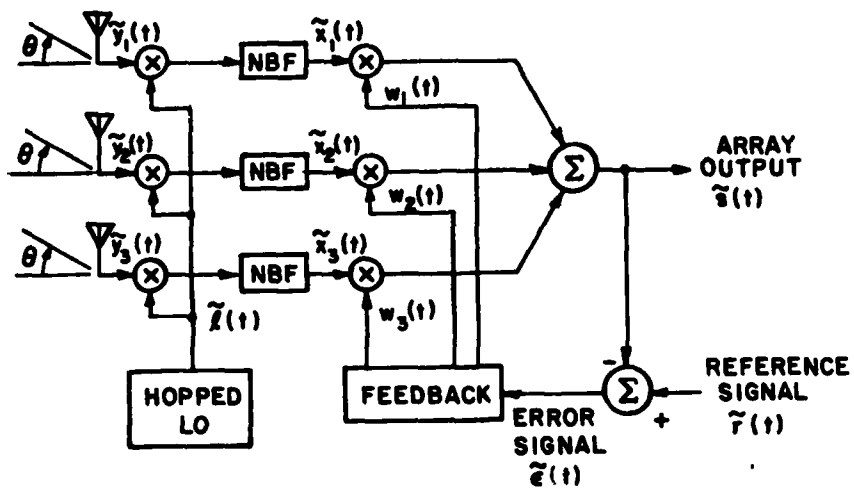


Figure 1. A Three-Element Adaptive Array.

and let $X(t)$ be a vector containing the signals at the LMS processor input

$$X(t) = [\tilde{x}_1(t), \tilde{x}_2(t), \tilde{x}_3(t)]^T, \quad (2)$$

where T denotes the transpose. We assume below that the array receives a desired signal and an interference signal, and that there is also thermal noise in the element outputs. Thus, $Y(t)$ and $X(t)$ may be written

$$Y(t) = Y_d(t) + Y_i(t) + Y_n(t), \quad (3)$$

and

$$X(t) = X_d(t) + X_i(t) + X_n(t), \quad (4)$$

where $Y_d(t)$, $Y_i(t)$ and $Y_n(t)$ are vectors containing the desired, interference and thermal noise signals from the elements, and $X_d(t)$, $X_i(t)$ and $X_n(t)$ are the corresponding vectors at the processor input.

Now let us define the signals and determine these vectors. First, we assume the desired signal is frequency hopped with a periodic hopping pattern. We suppose the hopping sequence repeats after p hops. We model the desired signal as a CW signal with constant frequency ω_h on each hop interval $T_{h-1} < t < T_h$, where h is an integer denoting the hop interval ($1 < h < p$) and T_h is the time at the end of interval h . The duration of hop interval h , $T_h - T_{h-1}$, is called the dwell time. We assume the dwell time is the same for each h . We refer to the separation between two ω_h that are adjacent in frequency as the

frequency spacing, and we assume the ω_h are equally spaced across the band. (Two ω_h that occur sequentially in a given hopping pattern are not necessarily adjacent.) We define the hopping frequency f_H to be the number of hops per second (the reciprocal of the dwell time), $f_H = (T_1 - T_0)^{-1}$, and the pattern frequency f_p to be the number of complete hopping periods (or "patterns") per second, i.e., $f_p = (T_p - T_0)^{-1} = f_H/p$. We define the center frequency ω_c of the desired signal to be the arithmetic mean of the hopping frequencies ω_h . (The antenna elements in Figure 1 are assumed to be a half wavelength apart at frequency ω_c .) We denote the difference between a specific signal frequency ω_h and the center frequency ω_c by $\Delta\omega_h$.

$$\Delta\omega_h = \omega_h - \omega_c \quad (5)$$

Finally, we define the relative bandwidth B_r of the desired signal to be its total bandwidth divided by its center frequency,

$$B_r = \frac{\max\{\omega_h\} - \min\{\omega_h\}}{\omega_c} \quad (6)$$

To dehop the desired signal, we assume the LO in Figure 1 is hopped synchronously with the received desired signal*. The LO signal is

*We do not address the issue of timing synchronization here. Also, if the desired signal arrives from a direction other than broadside, its hopping will have a different timing on each element, because of the propagation time delay between elements. Thus, strictly speaking, the LO hopping cannot be synchronized exactly with the desired signal hopping on every element. However, we assume the interelement propagation time to be very small compared to the dwell time. In this case, differences in desired signal timing on different elements may be neglected.

$$\tilde{x}(t) = e^{j(\omega_L + \Delta\omega_h)t} ; T_{h-1} < t < T_h , \quad (7)$$

where ω_L is the center frequency of the LO. We assume that $\omega_L < \omega_c$ and that the NBF has a center frequency $\omega_c - \omega_L$. The bandwidth of the NBF, which we denote by B_f , is assumed smaller than the separation between adjacent hopping frequencies. All the NBFs in Figure 1 are assumed identical.

With this model, the vector $Y_d(t)$ is

$$Y_d(t) = A_d \begin{matrix} e^{j[(\omega_c + \Delta\omega_h)t + \psi_d]} \\ e^{j[(\omega_c + \Delta\omega_h)(t - T_d) + \psi_d]} \\ e^{j[(\omega_c + \Delta\omega_h)(t - 2T_d) + \psi_d]} \end{matrix} ; T_{h-1} < t < T_h , \quad (8)$$

where A_d is the desired signal amplitude, ψ_d is the desired signal carrier phase angle, and T_d is the propagation time delay between two adjacent elements,

$$T_d = \frac{\pi}{\omega_c} \sin \theta_d . \quad (9)$$

θ_d is the desired signal arrival angle with respect to broadside. (θ is defined in Figure 1.) ψ_d is assumed to be a random variable uniformly distributed on $(0, 2\pi)$.

After dehoping, the desired signal vector $X_d(t)$ is

$$X_d(t) = A_d e^{j[(\omega_c - \omega_L)t + \psi_d]} U_d(t) ; T_{h-1} < t < T_h , \quad (10)$$

where

$$U_d(h) = [1, e^{-j\phi_d(h)}, e^{-j2\phi_d(h)}]^T, \quad (11)$$

and $\phi_d(h)$ is the desired signal interelement phase shift during interval h ,

$$\phi_d(h) = (\omega_c + \Delta\omega_h) T_d. \quad (12)$$

Next, consider the interference. Suppose the interference is a CW signal at frequency ω_i incident on the array from angle θ_i . The interference signal vector $Y_i(t)$ is

$$Y_i(t) = A_i \begin{bmatrix} e^{j[\omega_i t + \psi_i]} \\ e^{j[\omega_i(t-T_1) + \psi_i]} \\ e^{j[\omega_i(t-2T_1) + \psi_i]} \end{bmatrix}, \quad (13)$$

where A_i is the amplitude, ψ_i is the carrier phase angle and T_1 is the propagation time delay between two adjacent elements,

$$T_1 = \frac{\pi}{\omega_c} \sin \theta_i. \quad (14)$$

The carrier phase angle ψ_i is assumed uniformly distributed on $(0, 2\pi)$ and statistically independent of ψ_d .

After mixing and filtering, the interference signal vector $X_i(t)$ is

$$X_i(t) = A_i'(h) e^{j[(\omega_i - \omega_c - \Delta\omega_h)t + \psi_i]} U_i; \quad T_{h-1} < t < T_h, \quad (15)$$

where

$$A_i'(h) = \begin{cases} A_i : |\omega_i - \omega_c - \Delta\omega_{\eta}| < \frac{B_f}{2} , \\ 0 : \text{otherwise} \end{cases} \quad (16)$$

and

$$U_i = [1, e^{-j\phi_i}, e^{-j2\phi_i}]^T \quad (17)$$

with ϕ_i the interelement phase shift,

$$\phi_i = \frac{\omega_i}{\omega_c} \pi \sin \theta_i . \quad (18)$$

Note that the frequency hopping has converted the CW interference signal at the antenna element into a pulsed signal at the processor input.

Finally, we assume the element signals $\tilde{y}_j(t)$ contain white, gaussian noise. After mixing and filtering, the $\tilde{x}_j(t)$ then contain narrowband gaussian noise signals. The noise vector $X_n(t)$ is

$$X_n(t) = [\tilde{n}_1(t), \tilde{n}_2(t), \tilde{n}_3(t)]^T \quad (19)$$

where the $\tilde{n}_j(t)$ are zero mean, gaussian random processes, each with variance σ^2 . We assume the $\tilde{n}_j(t)$ are statistically independent of each other and of ψ_d and ψ_i .

Once the signal vector $X(t)$ is defined, the array weights may be found as follows. The weights satisfy the system of equations [1],

$$\frac{dW(t)}{dt} + k\phi(t)W(t) = kS(t) \quad (20)$$

where $W(t)$ is the weight vector

$$W(t) = [w_1(t), w_2(t), w_3(t)]^T, \quad (21)$$

k is the LMS loop gain, $\phi(t)$ is the covariance matrix,

$$\phi(t) = E[X^*(t)X^T(t)], \quad (22)$$

and $S(t)$ is the reference correlation vector,

$$S(t) = E[X^*(t)\tilde{r}(t)]. \quad (23)$$

In these equations, $E(\cdot)$ denotes expectation and $*$ complex conjugate.

Since $X_d(t)$, $X_f(t)$ and $X_n(t)$ are uncorrelated with each other, $\phi(t)$ reduces to

$$\begin{aligned} \phi(t) &= E[X_d^*(t)X_d^T(t)] + E[X_f^*(t)X_f^T(t)] + E[X_n^*(t)X_n^T(t)] \\ &= A_d^2 U_d^*(h)U_d^T(h) + A_f^2 U_f^*(h)U_f^T(h) + \sigma^2 I; \quad T_{h-1} < t < T_h. \end{aligned} \quad (24)$$

To find the reference correlation vector $S(t)$, we must define the reference signal $\tilde{r}(t)$. As discussed above, $\tilde{r}(t)$ must be a signal correlated with $X_d(t)$ and uncorrelated with $X_f(t)$ and $X_n(t)$. We shall assume the reference signal has the same form as the desired signal on channel 1 of the processor, but with amplitude A_r ,

$$\tilde{r}(t) = A_r e^{j[(\omega_c - \omega_L)t + \psi_d]}; \quad T_{h-1} < t < T_h. \quad (25)$$

Then, from (23), $S(t)$ is

$$S(t) = A_r A_d U_d^*(h) . \quad (26)$$

Also, we note that $\phi(t)$ and $S(t)$ depend only on h , because they are constant during each hop interval. Hence we denote their values during interval h by $\phi(h)$ and $S(h)$.

Thus, for one period of the hopping pattern, $W(t)$ satisfies the sequence of equations,

$$\begin{aligned} \frac{dW(t)}{dt} + k\phi(1)W(t) &= kS(1) ; T_0 < t < T_1 \\ \frac{dW(t)}{dt} + k\phi(2)W(t) &= kS(2) ; T_1 < t < T_2 \\ &\vdots \\ \frac{dW(t)}{dt} + k\phi(p)W(t) &= kS(p) ; T_{p-1} < t < T_p . \end{aligned} \quad (27)$$

Suppose $W(T_{h-1})$ is the value of $W(t)$ at the end of interval $h-1$. Then, since $W(t)$ is continuous at each hop, $W(T_{h-1})$ is also the initial value of $W(t)$ for interval h . Hence, the solution to this sequence of equations is*

$$\begin{aligned} W(t) &= e^{-k\phi(1)(t-T_0)} [W(T_0) - \phi^{-1}(1)S(1)] + \phi^{-1}(1)S(1); T_0 < t < T_1 \\ W(t) &= e^{-k\phi(2)(t-T_1)} [W(T_1) - \phi^{-1}(2)S(2)] + \phi^{-1}(2)S(2); T_1 < t < T_2 \end{aligned}$$

*Matrix exponentials, such as $e^{-k\phi(1)(t-T_0)}$, are defined in [10].

$$\begin{aligned}
 & \cdot \\
 & \cdot \\
 & \cdot \\
 W(t) = e^{-k\phi(p)(t-T_{p-1})} & [W(T_{p-1}) - \phi^{-1}(p)S(p)] + \phi^{-1}(p)S(p); T_{p-1} < t < T_1
 \end{aligned}
 \tag{28}$$

where $W(T_0), W(T_1), \dots, W(T_{p-1})$ are the initial weight vectors for each interval. If these initial vectors were known, we could calculate $W(t)$ at any other time from these equations.

To determine the $W(T_h)$, we proceed as follows. Because the hopping pattern is periodic, $\phi(t)$ and $S(t)$ are both periodic functions of time. Thus, $W(t)$ satisfies a differential equation with periodic coefficients and a periodic driving term. The solution to such an equation will also be a periodic function of time after any initial transients have died out.* In this paper we concentrate on the periodic steady-state behavior of $W(t)$. We do not consider initial transients. Once $W(t)$ has settled into its periodic steady-state, the initial weight vectors $W(T_0), W(T_1), \dots, W(T_{p-1})$ may be found by invoking the periodicity of $W(t)$ to note that $W(T_p)$ must be the same as $W(T_0)$. Thus, using (28) to compute $W(t)$ at the end of each interval, we have the following relations among the initial vectors $W(T_h)$,

$$W_1 = e^{-k\phi(1)(T_1-T_0)} [W_0 - \phi^{-1}(1)S(1)] + \phi^{-1}(1)S(1)$$

*This statement can be proven in the same manner as in Eqs. (24) - (29) of [11]. A general proof of this property of differential equations may be found in D'Angelo [12].

$$\begin{aligned}
W_2 &= e^{-k\phi(2)(T_2-T_1)} [W_1 - \phi^{-1}(2)S(2)] + \phi^{-1}(2)S(2) \\
&\vdots \\
W_{p-1} &= e^{-k\phi(p-1)(T_{p-1}-T_{p-2})} [W(T_{p-2}) - \phi^{-1}(p-1)S(p-1)] + \phi^{-1}(p-1)S(p-1) \\
W_0 &= e^{-k\phi(p)(T_p-T_{p-1})} [W_{p-1} - \phi^{-1}(p)S(p)] + \phi^{-1}(p)S(p), \quad (29)
\end{aligned}$$

where, to simplify notation, we have used $W_i = W(t_i)$. Note that in the last equation we have replaced W_p by W_0 . If the initial vectors W_i in (29) are regarded as unknowns, (29) has as many equations as unknowns. Rearranging (29) gives the following system of equations for the W_i .

$$\begin{bmatrix}
I & 0 & \dots & \dots & \dots & -e^{-k\phi(p)(T_p-T_{p-1})} \\
-e^{-k\phi(1)(T_1-T_0)} & I & & & & \\
0 & -e^{-k\phi(2)(T_2-T_1)} & & & & \\
\vdots & \vdots & \ddots & & & \\
\vdots & \vdots & \vdots & \ddots & & \\
0 & 0 & -e^{-k\phi(p-1)(T_{p-1}-T_{p-1})} & & & \\
\vdots & \vdots & \vdots & \ddots & & \\
0 & 0 & -e & & & I
\end{bmatrix}
\begin{bmatrix}
W_0 \\
\vdots \\
W_1 \\
\vdots \\
\vdots \\
\vdots \\
W_{p-1}
\end{bmatrix}$$

$$= \begin{bmatrix} [I - e^{-k\phi(p)(T_p - T_{p-1})}]_{\phi^{-1}(p)} S(p) \\ [I - e^{-k\phi(1)(T_1 - T_0)}]_{\phi^{-1}(1)} S(1) \\ \cdot \\ \cdot \\ [I - e^{-k\phi(p-1)(T_{p-1} - T_{p-2})}]_{\phi^{-1}(p-1)} S(p-1) \end{bmatrix} \quad (30)$$

This system may be solved numerically* for the initial vectors $W_j = W(T_j)$, and $W(t)$ may then be found for other times from (28).

Once the weights have been found, the array performance may be calculated. First, the time varying weights cause the array to modulate the desired signal. The desired signal at the array output is

$$\tilde{s}_d(t) = W^T(t) X_d(t) \quad , \quad (31)$$

or, from (10),

$$\tilde{s}_d(t) = A_d W^T(t) U_d(h) e^{j[(\omega_c - \omega_L)t + \psi_d]} ; \quad T_{h-1} < t < T_h \quad . \quad (32)$$

To characterize the desired signal modulation, we define the envelope modulation $a_d(t)$ and the phase modulation $\eta_d(t)$ by

To solve (30), one must evaluate matrix exponentials such as $e^{k\phi(1)(T_1 - T_0)}$. These may be computed by means of Sylvester's Theorem [13], according to the procedure discussed in [11], Eqs. (47) - (55).

$$a_d(t) = A_d |W^T(t)U_d(h)| ; T_{h-1} < t < T_h \quad (33)$$

and

$$n_d(t) = \langle W^T(t)U_d(h) \rangle ; T_{h-1} < t < T_h \quad (34)$$

The output signal powers also vary with time. The output desired signal power is

$$P_d = \frac{1}{2} E[|\tilde{s}_d(t)|^2] = \frac{1}{2} A_d^2 |W^T(t)U_d(h)|^2 ; T_{h-1} < t < t_h , \quad (35)$$

the output interference power is

$$P_i = \frac{1}{2} A_i'^2(h) |W^T(t)U_i|^2 ; T_{h-1} < t < T_h , \quad (36)$$

and the output thermal noise power is

$$P_n = \frac{\sigma^2}{2} |W(t)|^2 . \quad (37)$$

The output SINR is

$$SINR = \frac{P_d}{P_i + P_n} = \frac{\epsilon_d |W^T(t)U_d(h)|^2}{|W(t)|^2 + \epsilon_i'(h) |W^T(t)U_i|^2} ; T_{h-1} < t < T_h \quad (38)$$

where ϵ_d is the input SNR per element,

$$\epsilon_d = \frac{A_d^2}{\sigma} , \quad (39)$$

$\epsilon_i'(h)$ is the input INR in each processor channel during interval h ,

$$\xi_i'(h) = \begin{cases} \xi_i : |\omega_i - \omega_c - \Delta\omega_h| < \frac{B_f}{2} \\ 0 : \text{otherwise} \end{cases} \quad (40)$$

and ξ_i is

$$\xi_i = \frac{A_i^2}{\sigma} \quad (41)$$

In Section III we refer to ξ_i as the "input INR". The reader will understand that ξ_i is actually the INR on each processor channel only for those hopping intervals when the interference appears in the filter output.

In Section III we use these equations to calculate the array performance with frequency hopped signals.

III. RESULTS

Using the equations above, we have computed the signal modulation and the SINR for a variety of cases. We present these results as follows. First, in Part A, we show typical curves of the desired signal envelope and phase modulation and the output SINR as functions of time. To characterize these time-varying quantities in a simple way, we also define an envelope variation, a phase variation and a bit error probability. Then, in Parts B - F, we describe how each signal parameter affects the envelope and phase variations and the bit error probability. Part B discusses hopping frequency, Part C frequency jump size, Part D interference frequency, Part E arrival angles and Part F signal powers.

A. Typical Curves

First we consider envelope modulation. Figure 2 is a typical curve, computed for $\theta_d = 15^\circ$, $\theta_f = 30^\circ$, $\xi_d = 6\text{dB}$, $\xi_f = 20\text{dB}$, $B_r = 0.1$ and $p = 2$. The figure shows the output desired signal envelope versus time. The envelope is plotted in dB, relative to the envelope that would exist with no frequency hopping and no interference. The time axis is normalized so a complete hopping period begins at $t = 0$ and ends at $t = 1$. The desired signal is on frequency $\omega_1 = 0.95\omega_c$ for $0 < t < 1/2$ and on frequency $\omega_2 = 1.05\omega_c$ for $1/2 < t < 1$. The interference is on frequency ω_1 (i.e., $\omega_1 = 0.95\omega_c$). As may be seen, there is significant envelope modulation on the output desired signal.

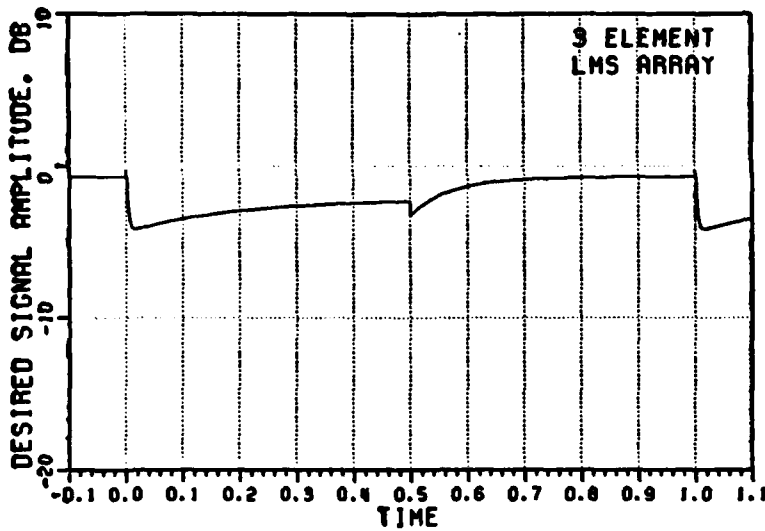


Figure 2. Desired Signal Amplitude vs. Time
 $\theta_d = 15^\circ$, $\theta_1 = 30^\circ$, $\xi_d = 6$ dB, $\xi_1 = 20$ dB.
 $p = 2$, $B_r = 0.1$, $\omega_1 = \omega_1$.

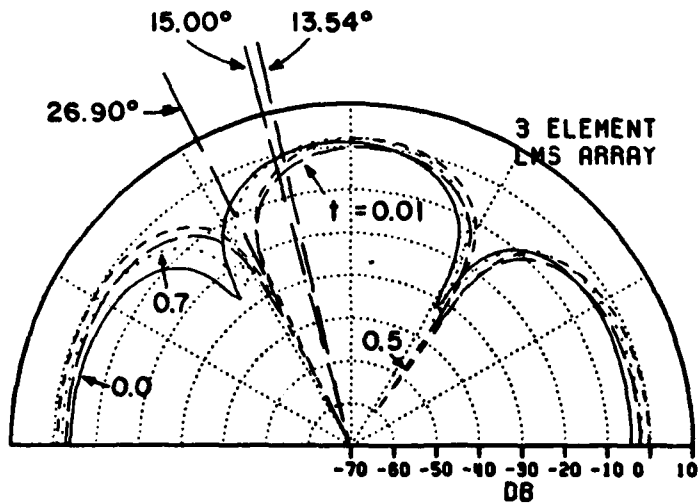


Figure 3. Array Patterns During Hopping Period
 $\theta_d = 15^\circ$, $\theta_1 = 30^\circ$, $\xi_d = 6$ dB, $\xi_1 = 20$ dB.
 $p = 2$, $B_r = 0.1$, $\omega_1 = \omega_1$. Patterns computed at ω_2 .

Moreover, step discontinuities occur in the envelope when the frequency jumps.

The reason for this behavior is as follows. A jump in desired signal frequency, at a given arrival angle, is electrically equivalent to a jump in desired signal arrival angle with no change in frequency, because either situation causes a jump in the interelement phase shift. In Figure 2, the desired signal arrives from $\theta = 15^\circ$ with frequency $0.95\omega_c$ for $0 < t < 1/2$ and $1.05\omega_c$ for $1/2 < t < 1$. This situation is electrically the same as if the desired signal were always on a frequency $1.05\omega_c$ and arrived from $\theta = 13.54^\circ$ for $0 < t < 1/2$ and from $\theta = 15^\circ$ for $1/2 < t < 1$. Figure 3 shows the pattern of the array computed at frequency $1.05\omega_c$ for several times during the hopping period. The interference is at $\theta = 30^\circ$ on frequency $.95\omega_c$, which is equivalent to interference arriving from $\theta = 26.9^\circ$ at frequency $1.05\omega_c$. As may be seen in Figure 3, at the end of interval 1 (at $t = 1/2$), the array has formed a null on the interference at $\theta = 26.9^\circ$. In the second hop interval, the interference disappears (it is filtered out) and the desired signal angle jumps from 13.54° to 15° . Because this jump is toward the existing null, an instantaneous drop in the desired signal amplitude occurs at the beginning of interval 2. During interval 2, the desired signal amplitude increases as the array adapts. Then at the end of interval 2, the desired signal angle jumps back from 15° to 13.54° (away from the null), so the desired signal amplitude jumps up instantaneously. After this jump, the desired signal amplitude drops as the weights form the null at 26.9° again, since the interference has

reappeared at 26.9° during interval 1.

In order to characterize such a time varying waveform in a simple way for use below, we define an envelope variation as follows. Let a_{\max} be the largest and a_{\min} be the smallest (absolute) value of the output desired signal envelope during the hopping period. Then let

$$m = \frac{a_{\max} - a_{\min}}{a_{\max}} . \quad (42)$$

m is the fractional modulation, since it is the total excursion of the envelope normalized to its peak. We refer to m as the envelope variation.

Next we consider phase modulation. Figure 4 shows a typical curve of output desired signal phase versus time, for the case $\theta_d = 15^\circ$, $\theta_i = 45^\circ$, $\xi_d = 6\text{dB}$, $\xi_i = 20\text{ dB}$, $B_r = 0.5$, $p = 2$ and $\omega_i = \omega_1$. As may be seen, there is substantial phase modulation on the output desired signal. Figure 4 is typical of what usually happens: the desired signal phase jumps up or down at the beginning of each hop interval and then decays back to zero.

This phase modulation is due to the frequency hopping on the desired signal and not to the presence of interference. Figure 5 shows the output desired signal phase versus time for the same situation as in Figure 4 but without interference. Note that almost the same phase modulation occurs in both cases. The phase modulation occurs because the desired signal interelement phase shift jumps when the frequency hops (unless the signal is incident from broadside). Hence, immediately after each hop, the array weights no longer have the correct phasing

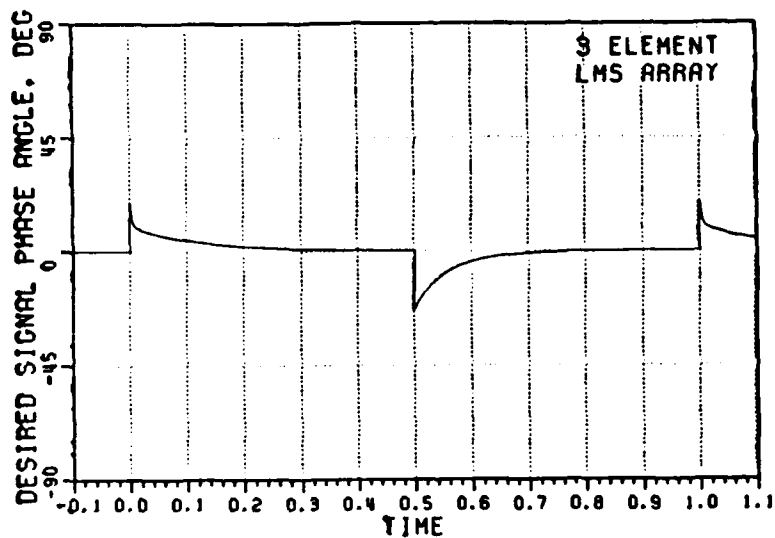


Figure 4. Desired Signal Phase Angle vs. Time
 $\theta_d = 15^\circ$, $\theta_i = 45^\circ$, $\epsilon_d = 6$ dB, $\epsilon_i = 20$ dB,
 $p = 2$, $B_r = 0.5$, $\omega_i = \omega_1$.

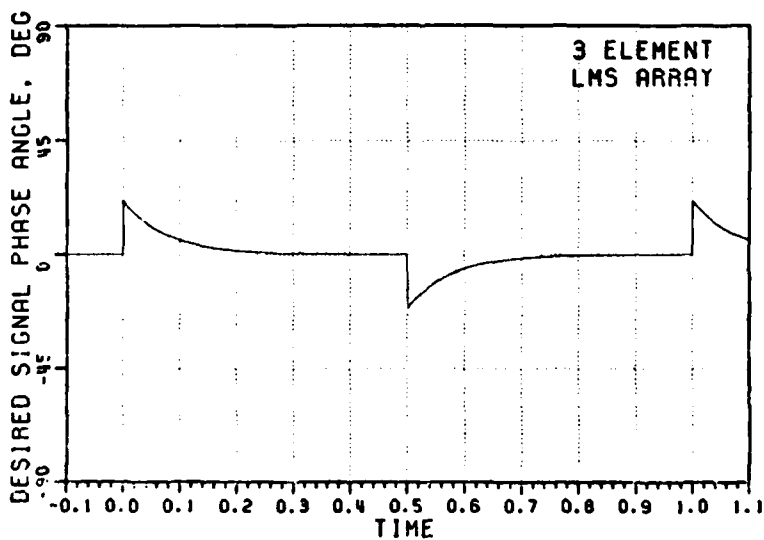


Figure 5. Desired Signal Phase Angle vs. Time
 $\theta_d = 15^\circ$, $\epsilon_d = 6$ dB, $p = 2$, $B_r = 0.5$, no interference.

to maximize desired signal response. As the weights respond after each hop, the phase shift of the array seen by the desired signal changes with time.

To characterize phase modulation, we define η_{\max} and η_{\min} to be the maximum and minimum phase angles of the output desired signal over the hopping period ($-\pi < \eta_{\min} < \eta_{\max} < 2\pi$) and β to be

$$\beta = \frac{\eta_{\max} - \eta_{\min}}{2\pi} . \quad (43)$$

We refer to β as the phase variation.

Finally, we consider the output SINR from the array. Figure 6 shows a typical curve of SINR versus time over one hopping period. This curve is computed for the same parameters as in Figure 2. Note that the SINR drops approximately 16 dB at the beginning of the hopping period. Although the SINR recovers quickly from this drop, such a drop can nevertheless greatly increase the bit error probability for the received signal, since the number of bit detection errors is larger by orders of magnitude during this short interval than it is when the SINR is higher.

To characterize such a time-varying SINR curve, we define an average bit error probability. We arbitrarily assume that the desired signal, in addition to being frequency hopped, has binary DPSK

(different phase shift keyed) modulation*[14]. The bit error probability for a DPSK signal in white noise is [15]

$$P_e = \frac{1}{2} e^{-E_b/N_0} , \quad (44)$$

where E_b is the signal energy per bit and N_0 is the one-sided thermal noise spectral density. For our purposes, we may replace E_b/N_0 by signal-to-noise ratio,

$$\frac{E_b}{N_0} = \frac{P_d T_b}{N_0} = \frac{P_d}{(N_0/T_b)} = \text{SNR} , \quad (45)$$

where P_d is the desired signal power and T_b is the bit duration. I.e., since T_b^{-1} is the effective noise bandwidth, N_0/T_b is the noise power. Hence P_e may be written

$$P_e = \frac{1}{2} e^{-\text{SNR}} . \quad (46)$$

In addition, for this analysis we shall assume that interference power has the same effect on detector performance as thermal noise power, so

*Adding biphase modulation to the desired signal does not change the array weight behavior as long as the bandwidth of the phase modulation is small enough to pass through the dehoppping filters. With small bandwidth, the covariance matrix $\phi(t)$ is the same as for a CW signal because the phase modulation terms cancel out. (Also, aside from the dehoppping filters, it has been shown [16] that desired signal bandwidth has almost no effect on array performance anyway, even if the bandwidth is large.) Moreover, as long as the reference signal carries the same DPSK modulation as the desired signal, which we assume, the reference correlation vector $S(t)$ is also unchanged. Since both $\phi(t)$ and $S(t)$ are the same, the weight behavior will be the same with this signal as with a CW signal. (Some examples of how digital phase modulation can be transferred to the reference signal may be found in [4 - 8].)

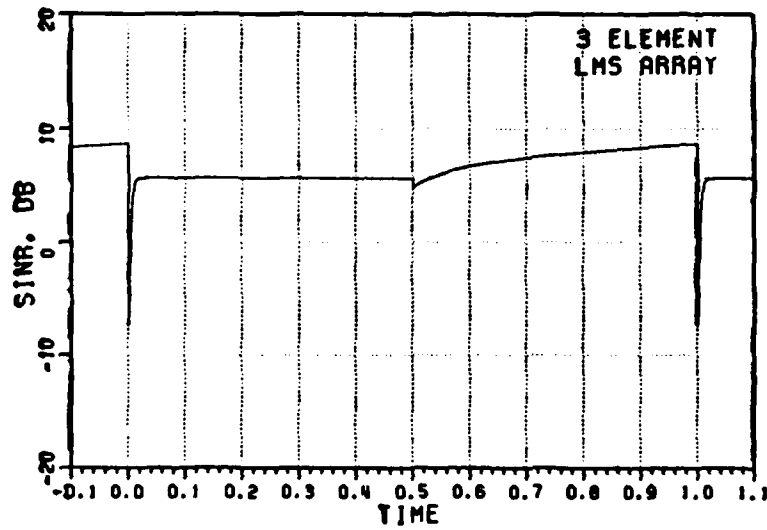


Figure 6. SINR vs. Time
 $\theta_d = 15^\circ$, $\theta_i = 30^\circ$, $\xi_d = 6$ dB, $\xi_i = 20$ dB,
 $p = 2$, $B_r = 0.1$, $\omega_i = \omega_1$.

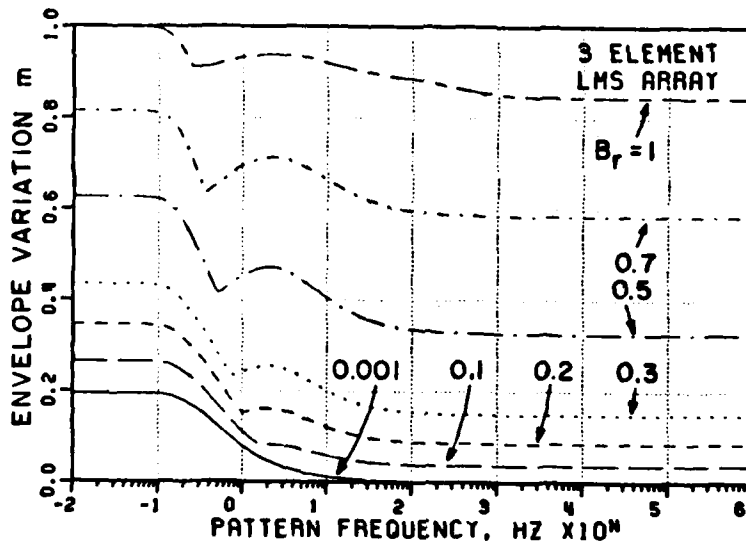


Figure 7. Envelope Variation vs. Pattern Frequency
 $\theta_d = 15^\circ$, $\theta_i = 45^\circ$, $\xi_d = 6$ dB, $\xi_i = 40$ dB,
 $p = 2$, $\omega_i = \omega_1$.

$$P_e = \frac{1}{Z} e^{-\text{SINR}} \quad (47)$$

Finally, we assume that the SINR transients and the desired signal phase modulation produced by the array are slow compared to the bit length T_b . In this case the SINR and the signal phase may be considered constant over a time interval of $2T_b$. (Two adjacent bits are used to detect a DPSK signal.) We define the effective bit error probability \bar{P}_e as the average of P_e over one hopping period,

$$\bar{P}_e = \frac{1}{T_p - T_p} \int_{T_0}^{T_p} \frac{1}{Z} e^{-\text{SINR}(t)} dt \quad (48)$$

We use (48) below for comparing different SINR curves*.

Now let us consider the effect of the various signal parameters on the signal modulation and the bit error probability.

B. The Effect of Hopping Frequency

The envelope and phase variations m and β are large at low hopping frequency and drop as the frequency increases. Bit error probability, on the other hand, is low at low frequency and increases with frequency. Both m and \bar{P}_e may have local peaks at intermediate frequencies.

Figure 7 shows typical curves of m versus (pattern) frequency.

*We recognize that (48) glosses over many subtleties that will affect detector performance in an actual system. Our intent here is simply to reduce each SINR curve to a single number to compare different SINR curves. In the absence of a specific system definition, (48) will do as well as anything.

This set of curves was computed for $\theta_d = 15^\circ$, $\theta_f = 45^\circ$, $\xi_d = 6$ dB, $\xi_f = 40$ dB, $p = 2$ and $\omega_f = \omega_1$. The figure shows several curves for different hopping bandwidths B_f . As may be seen, for all but the smallest bandwidths, m has a complicated behavior at intermediate frequencies. This behavior occurs because of the way the desired signal envelope changes as the hopping frequency varies. In particular, the time at which a_{\min} occurs is in one hopping interval for low values of f_p and in the other hopping interval for high values of f_p . Typically the smallest envelope in one interval increases with f_p , while the smallest envelope in the other interval decreases with f_p . At the value of f_p where the two minima become equal, the location of a_{\min} in time changes from one hop interval to the other. At this change, the slope of a_{\min} versus f_p reverses, so the slope of m changes in Figure 10.

Figure 8 shows typical curves of phase variation β versus f_p . These curves were computed for the same parameters as in Figure 7. In general, phase variation is highest at low hopping frequency and drops to a constant as the hopping frequency increases. At large f_p , the array weights are too slow to track the hopping. The nonzero asymptotic phase variation is caused by the jumps in interelement phase shift when the frequency hops.

Finally, Figure 9 shows typical curves of bit error probability \bar{P}_e versus f_p , again for the same parameters as in Figure 7. As may be seen, for higher bandwidths \bar{P}_e simply increases with f_p . At lower bandwidths, \bar{P}_e peaks at intermediate f_p and then drops at higher f_p . However, \bar{P}_e is always higher at large f_p than at low f_p . This

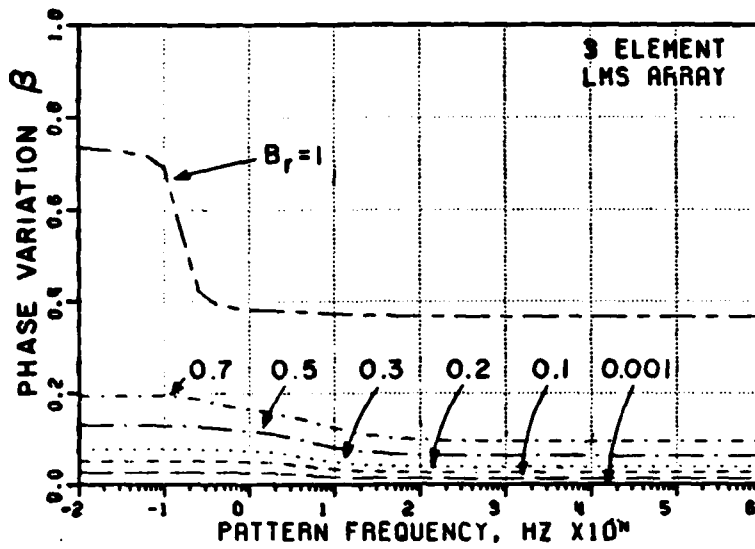


Figure 8. Phase Variation vs. Pattern Frequency
 $\theta_d = 15^\circ$, $\theta_f = 45^\circ$, $\epsilon_d = 6$ dB, $\epsilon_f = 40$ dB,
 $p = 2$, $\omega_f = \omega_1$.

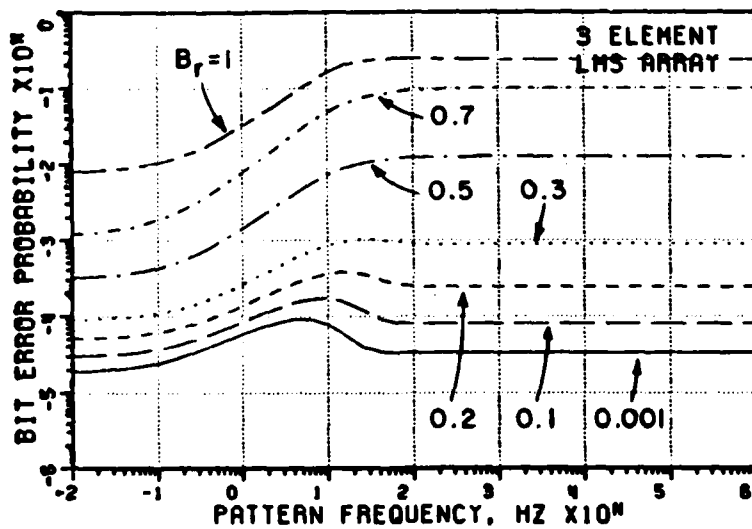


Figure 9. Bit Error Probability vs. Pattern Frequency
 $\theta_d = 15^\circ$, $\theta_f = 45^\circ$, $\epsilon_d = 6$ dB, $\epsilon_f = 40$ dB,
 $p = 2$, $\omega_f = \omega_1$.

behavior is similar to what happens when an adaptive array receives pulsed interference and a desired signal with no hopping [11]. (Frequency hopping converts the CW interference into pulsed interference. The two problems differ, however, because frequency hopping also causes jumps in the desired signal interelement phase shifts.)

C. The Effect of Frequency

The larger the frequency jumps encountered by the array, the larger the variations M and β and the greater the SINR reduction.

In a frequency hopped system, the size of the frequency jumps depends not only on the frequency spacing (the total bandwidth divided by the number of frequencies), but also on the hopping pattern. For the same spacing, different hopping patterns will produce different frequency jumps. Moreover, bit error probability is affected not only by the size of the frequency jumps, but also by how often the jumps occur, since it is an integrated quantity. In general, to minimize P_e , one should choose a hopping pattern that minimizes the number of large jumps and also reduces the frequency with which large jumps occur.

The effect of frequency jump size may be seen in Figures 7, 8 and 9. These figures each show several curves for different bandwidths B_T . Since there are only 2 frequencies ($p = 2$), the total bandwidth is the same as the frequency spacing and the frequency jump size. As may be seen, as bandwidth increases, the variation m and β and the bit error probability P_e all increase.

This behavior is easily understood. As the desired signal frequency jumps become larger, the jump in interelement phase shift at each hop becomes larger. A larger jump means that the array weights are farther from their optimal values at the new frequency. Thus, a larger weight transient is required after the jump. More envelope and phase modulation is produced and the SINR is lower after the jump.

D. The Effect of Interference Frequency

Interference near the edge of the hopping bandwidth is more harmful to the array than interference near the center of the band.

Figures 10 and 11 illustrate this point. These figures show \overline{P}_e versus f_p for $\theta_d = 15^\circ$, $\theta_i = 45^\circ$, $\epsilon_d = 6$ dB, $\epsilon_i = 40$ dB and $p = 3$. Figure 10 is for $\omega_i = \omega_1$ and Figure 11 is for $\omega_i = \omega_2$ (where $\omega_1 < \omega_2 < \omega_3$). The performance in Figure 10, when the interference is at the edge of the hopping band, is much worse than that in Figure 11, when the interference is at the center of the band. The reason for this difference may be understood in terms of the equivalence between desired signal frequency and arrival angle discussed earlier. Suppose $0 < \theta_d < \theta_i$ as in Figure 10. The array will produce a null in the pattern at θ_i on the interference frequency, either ω_1 or ω_2 . Since $0 < \theta_d < \theta_i$, the equivalent desired signal arrival angle, as seen on the interference frequency, will be closest to θ_i when the desired signal is on frequency ω_3 . The equivalent angle will be closer to θ_i if the interference is on ω_1 than if the interference is on ω_2 , since $\omega_3 - \omega_1$ is greater than $\omega_3 - \omega_2$. Hence, with interference on ω_1 , the desired

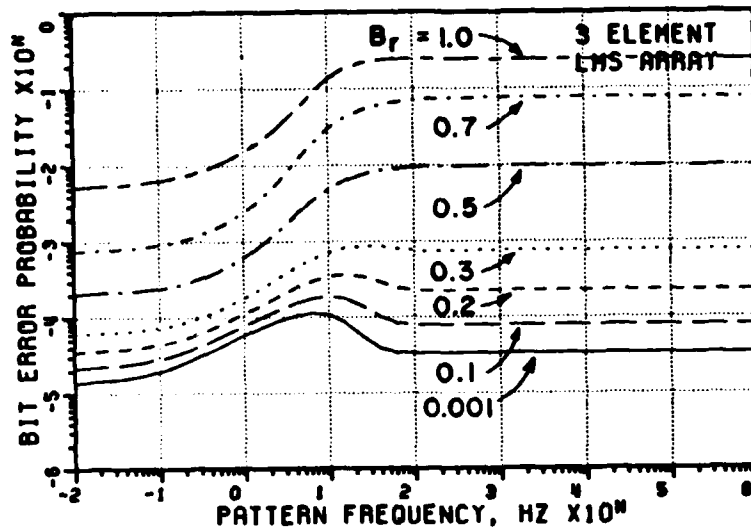


Figure 10. Bit Error Probability vs. Pattern Frequency
 $\theta_d = 15^\circ$, $\theta_i = 45^\circ$, $\xi_d = 6$ dB, $\xi_i = 40$ dB,
 $p = 3$, $\omega_i = \omega_1$.

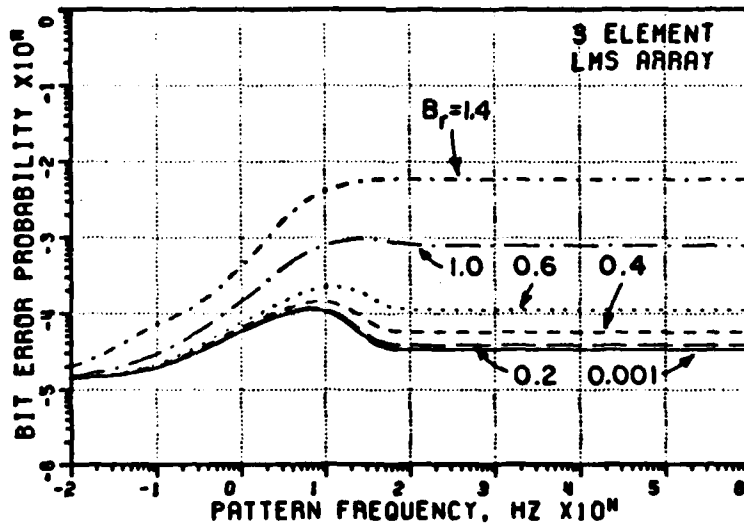


Figure 11. Bit Error-Probability vs. Pattern Frequency
 $\theta_d = 15^\circ$, $\theta_i = 45^\circ$, $\xi_d = 6$ dB, $\xi_i = 40$ dB,
 $p = 3$, $\omega_i = \omega_2$.

signal falls farther into the interference null, the SINR is reduced more and a higher P_e results than with interference on ω_2 .

Note that which edge of the band is worse depends on the signal arrival angles. In the example above, we have $0 < \theta_d < \theta_i$ and the worst performance is obtained with the interference on ω_1 . If instead we had $0 < \theta_i < \theta_d$, then interference on ω_3 , the other band edge, will give the worst performance.

E. The Effect of Arrival Angles

The envelope variation and the bit error probability increase as the interference arrival angle approaches the desired signal arrival angle. Interference arrival angle has almost no effect on phase modulation except when the interference signal is extremely close to the desired signal.

Figures 12 and 13 show the envelope variation m as a function of pattern frequency for $\theta_d = 15^\circ$, $\epsilon_d = 6$ dB, $\epsilon_i = 40$ dB, $B_r = 0.1$, $p = 2$, $\omega_i = \omega_1$ and for different interference angles. Figure 12 shows $\theta_i = 0^\circ, 30^\circ, 45^\circ, 60^\circ$ and 90° , and Figure 13 shows $\theta_i = 5^\circ, 10^\circ, 13^\circ, 17^\circ, 20^\circ$ and 25° . It may be seen that m increases as $|\theta_i - \theta_d|$ decreases. For θ_i very near θ_d , the variation m is quite large.

The phase variation β is small unless θ_i is very near θ_d . Figure 14 shows a typical case, for $\theta_d = 15^\circ$, $\epsilon_d = 6$ dB, $\epsilon_i = 40$ dB, $B_r = 0.5$, $p = 2$ and $\omega_i = \omega_1$. Note also that β is much larger for θ_i just above θ_d than for θ_i just below θ_d . The reason is as discussed above: in one

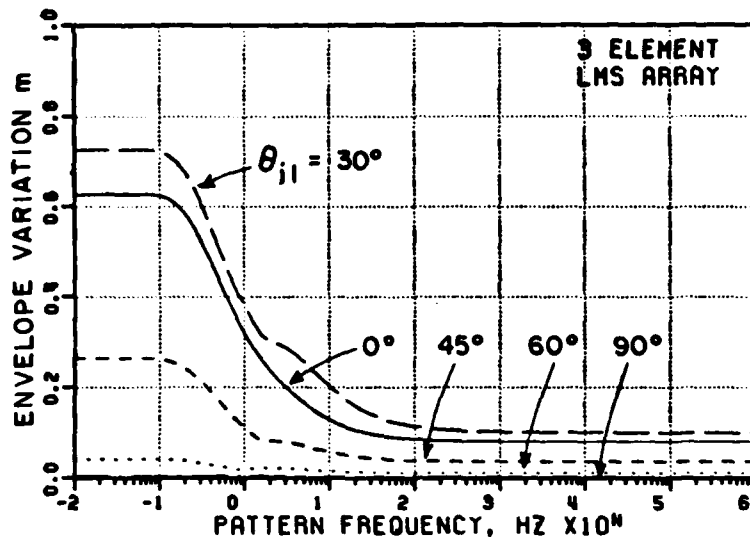


Figure 12. Envelope Variation vs. Pattern Frequency
 $\theta_d = 15^\circ$, $\epsilon_d = 6$ dB, $\epsilon_f = 40$ dB, $p = 2$,
 $B_r = 0.1$, $\omega_f = \omega_1$.

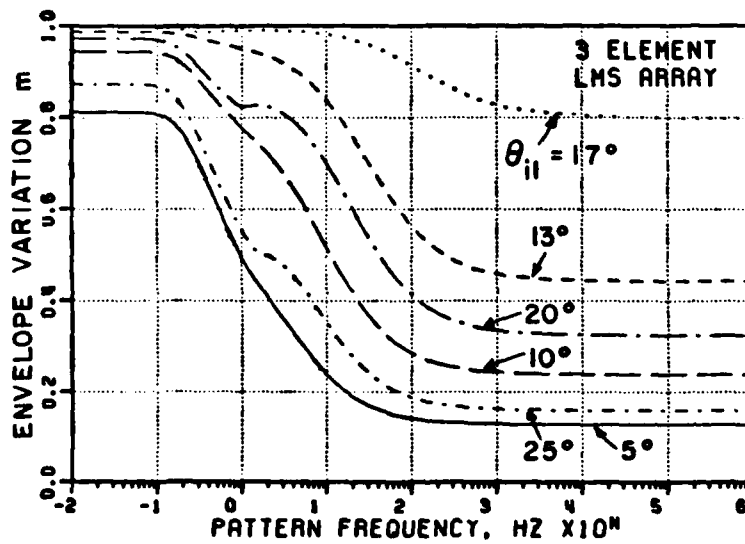


Figure 13. Envelope Variation vs. Pattern Frequency
 $\theta_d = 15^\circ$, $\epsilon_d = 6$ dB, $\epsilon_f = 40$ dB, $p = 2$,
 $B_r = 0.1$, $\omega_f = \omega_1$.

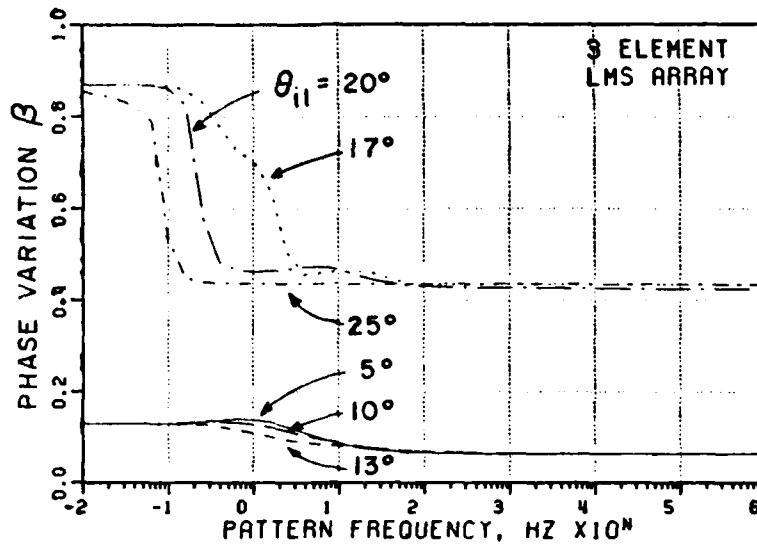


Figure 14. Phase Variation vs. Pattern Frequency
 $\theta_d = 15^\circ$, $\epsilon_d = 6$ dB, $\epsilon_j = 40$ dB, $p = 2$,
 $B_r = 0.5$, $\omega_j = \omega_1$.

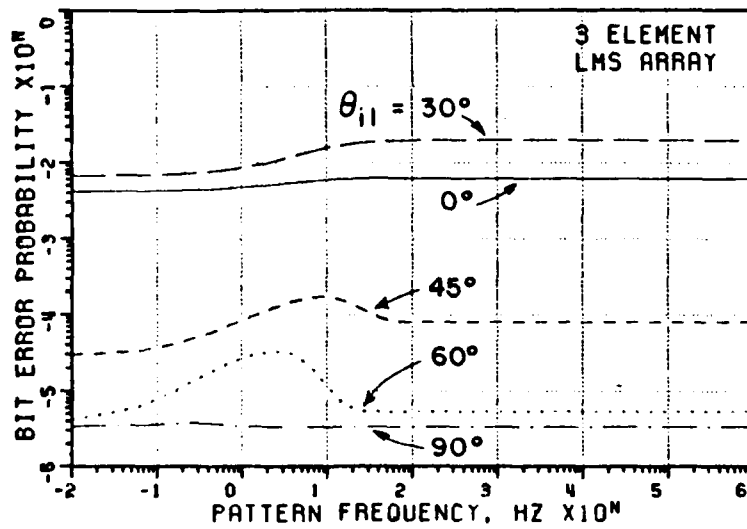


Figure 15. Bit Error Probability vs. Pattern Frequency
 $\theta_d = 15^\circ$, $\epsilon_d = 6$ dB, $\epsilon_j = 40$ dB, $p = 2$,
 $B_r = 0.1$, $\omega_j = \omega_1$.

case the desired signal hops into the null left by the interference whereas in the other it hops away from the null.

Figure 15 shows curves of the bit error probability for the same parameter values as in Figure 12. It is seen that \bar{P}_e is largest when θ_i is near θ_d .

F. The Effect of Signal Powers

The input INR has almost no effect on the phase modulation and very little effect on the envelope modulation. The effect of the INR on the bit error probability is primarily to shift the value of the hopping frequency for a given \bar{P}_e . Bit error probability is very sensitive to the input SNR.

Figures 16 and 17 show the envelope variation and the bit error probability versus f_p for $\theta_d = 15^\circ$, $\theta_i = 45^\circ$, $\xi_d = 6$ dB, $p = 2$, $\omega_i = \omega_1$, $B_r = 0.1$ and for several values of INR. Figure 17 illustrates how the hopping frequency at which \bar{P}_e peaks varies with the INR. Figure 18 shows β versus f_p for the same parameters as in Figures 16 and 17 except that $B_r = 0.5$.

Figure 19 shows the bit error probability versus f_p for $\theta_d = 15^\circ$, $\theta_i = 45^\circ$, $\xi_i = 40$ dB, $p = 2$, $\omega_i = \omega_1$, $B_r = 0.1$ and for several values of input SNR. As may be seen, \bar{P}_e is extremely sensitive to the SNR, as it would be even in a simple DPSK communication system without an adaptive array.

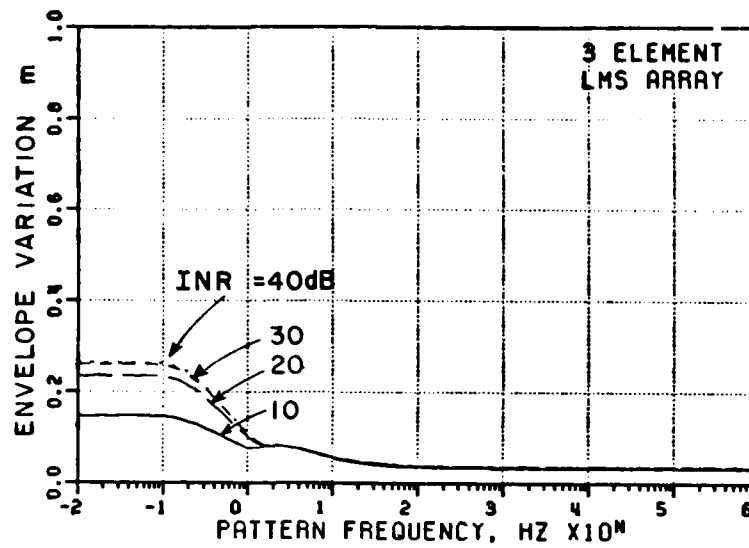


Figure 16. Envelope Variation vs. Pattern Frequency
 $\theta_d = 15^\circ$, $\theta_i = 45^\circ$, $\xi_d = 6$ dB, $p = 2$,
 $B_r = 0.1$, $\omega_i = \omega_1$.

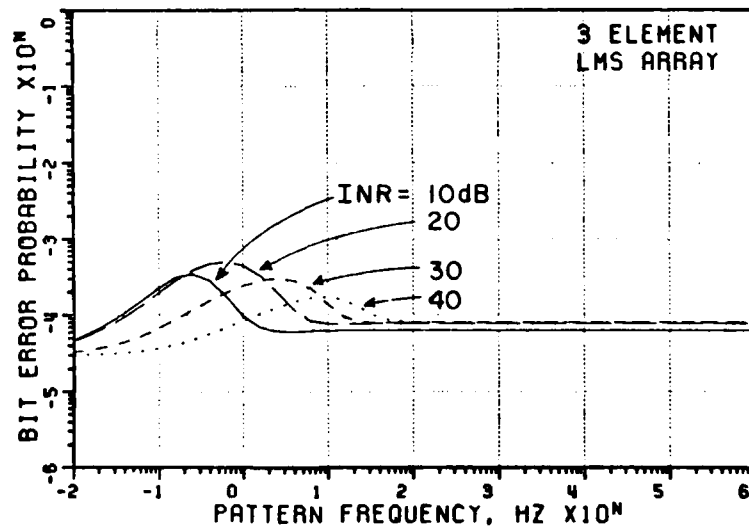


Figure 17. Bit Error Probability vs. Pattern Frequency
 $\theta_d = 15^\circ$, $\theta_i = 45^\circ$, $\xi_d = 6$ dB, $p = 2$,
 $B_r = 0.1$, $\omega_i = \omega_1$.

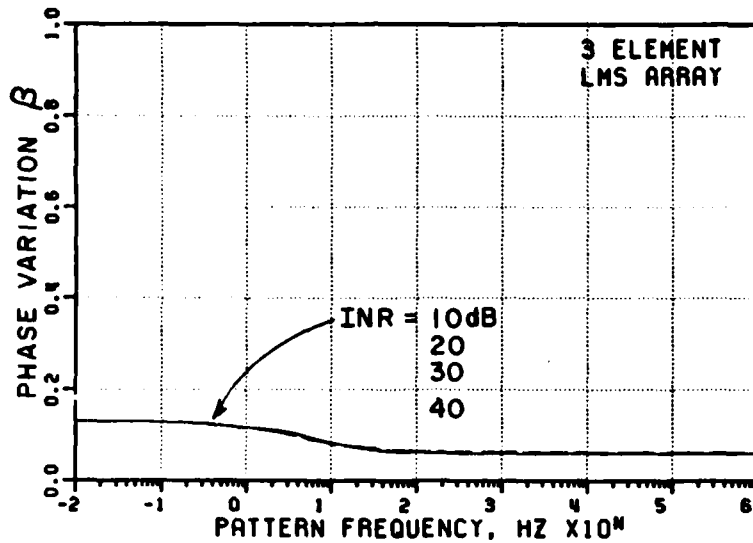


Figure 18. Phase Variation vs. Pattern Frequency
 $\theta_d = 15^\circ$, $\theta_i = 45^\circ$, $\epsilon_d = 6$ dB, $p = 2$,
 $B_r = 0.5$, $\omega_i = \omega_1$.

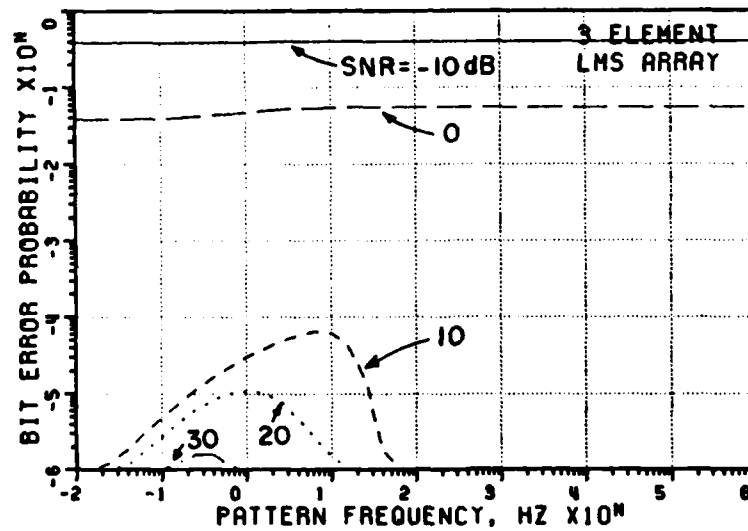


Figure 19. Bit Error Probability vs. Pattern Frequency
 $\theta_d = 15^\circ$, $\theta_i = 45^\circ$, $\epsilon_i = 40$ dB, $p = 2$,
 $B_r = 0.1$, $\omega_i = \omega_1$.

IV. CONCLUSIONS

A frequency hopped desired signal has several effects on an LMS array. It causes the array to modulate both the envelope and the phase of the output desired signal. Also, it causes the array output SINR to vary with time below its optimal value and increases the bit error probability for the received signal.

The signal parameters affect the desired signal modulation and the bit error probability as follows:

1. Envelope and phase modulation are large for low hopping frequencies and drop as the frequency increases. Bit error probability is low at low hopping frequencies and increases with frequency. Both the envelope variation and the bit error probability may have local peaks at intermediate hopping frequencies.
2. Envelope and phase modulation increase with the size of the frequency jumps in the hopping pattern. Bit error probability is increased as the frequency jump size increases.
3. An interference frequency at the edge of the hopping bandwidth is more harmful to the array performance than an interference frequency at the center of the band.
4. Envelope modulation and bit error probability increase as the interference arrival angle approaches the

desired signal arrival angle. Phase modulation is not affected by interference arrival angle unless the interference is extremely close to the desired signal.

5. Input INR has almost no effect on phase modulation and very little effect on envelope modulation. Input INR affects bit error probability by shifting the value of the hopping frequency required for a given bit error probability. Input SNR has a very large effect on bit error probability, as it would in any DPSK system, even without an adaptive array.

V. REFERENCES

1. B. Widrow, P.E. Mantev, L.J. Griffiths and B.B. Goode, "Adaptive Antenna Systems," Proc. IEEE, Dec. 1967, 55, 2143.
2. R.T. Compton, Jr., "An Experimental Four-Element Adaptive Array," IEEE Trans. on Antennas and Propagation, September 1976, AP-24, 697.
3. R.L. Riegler and R.T. Compton, Jr., "An Adaptive Array for Interference Rejection," Proc. IEEE, June 1973, 61, 748.
4. R.T. Compton, Jr., R.J. Huff, W.G. Swarner and A.A. Ksienski, "Adaptive Arrays for Communication Systems: An Overview of Research at the Ohio State University," IEEE Trans. on Antennas and Propagation, September 1976, AP-24, 599.
5. E.C. Hudson, "Use of an Adaptive Array in a Frequency-Shift Keyed Communication System," Report 712684-1, August 1980, The Ohio State University ElectroScience Laboratory, Columbus, OH 43212; prepared under Contract N00019-80-C-0181 for Naval Air Systems Command.
6. M.W. Ganz, "On the Performance of an Adaptive Array in a Frequency Shift Keyed Communication System," M.Sc. Thesis, 1982, Department of Electrical Engineering, The Ohio State University, Columbus, OH 43212.
7. R.T. Compton, Jr., "An Adaptive Array in a Spread Spectrum Communication System," Proc. IEEE, March 1978, 66, 289.
8. J.H. Winters, "Spread Spectrum in a Four-Phase Communication System Employing Adaptive Antennas," IEEE Trans. on Communications, May 1982, COM-30, 929.
9. R.C. Dixon, Spread Spectrum Systems, John Wiley and Sons, Inc., New York, 1976.
10. R. Bellman, Introduction to Matrix Analysis, McGraw-Hill Book Co., New York, 1970.
11. R.T. Compton, Jr., "The Effect of a Pulsed Interference Signal on an Adaptive Array," IEEE Trans. on Aerospace and Electronic Systems, May 1982, AES-18, 297.
12. H. D'Angelo, Linear Time-Varying Systems: Analysis and Synthesis, Allyn and Bacon, Boston, 1970.

13. F.B. Hildebrand, Methods of Applied Mathematics, Prentice-Hall, Inc., Englewood Cliffs, N.J., 1952.
14. R.E. Ziemer and W.H. Tranter, Principles of Communications, Houghton Mifflin, Inc., Boston, 1976.
15. W.C. Lindsey and M.K. Simon, Telecommunication Systems Engineering, Prentice-Hall, Inc., Englewood Cliffs, N.J., 1973.
16. W.E. Rodgers and R.T. Compton, Jr., "Adaptive Array Bandwidth with Tapped Delay-Line Processing," IEEE Trans. on Aerospace and Electronic Systems, January 1979, AES-15, 21.